

# Condensation Particle Counter Proportionality Calibration from 1 particle·cm<sup>-3</sup> to 10<sup>4</sup> particles·cm<sup>-3</sup>

Miles Owen, US Army Primary Standards Laboratory  
George Mulholland, University of Maryland at College Park  
Will Guthrie, National Institute of Standards and Technology, Gaithersburg Maryland, 20899

---

The linearity of a condensation particle counter (CPC) (3760A, TSI, Inc.) for a monodisperse aerosol has been previously evaluated by comparison to an aerosol electrometer (AE) (Fletcher et al., 2009). The comparison of the CPC to the AE is an absolute calibration of the CPC with traceability to SI units. However, due to the limitations of the AE, accurate measurements of aerosol concentration cannot be performed below approximately 1000 particles·cm<sup>-3</sup> for typical CPCs. Furthermore the linear model fit to the AE – CPC calibration data results in a statistically significant intercept (Fletcher et al., 2009), which causes discrepancies between the linear model and the CPC reading when extrapolated to lower concentrations. The presence of the intercept also introduces some reluctance to assume a proportional fit and extrapolate to zero. This creates problems for laboratories that require legal calibrations of CPCs at concentrations below 10<sup>3</sup> particles·cm<sup>-3</sup>. In this work a proportional statistical model for the CPC concentration is proposed, and an experimental method to verify the model and quantify the uncertainty of the fit over a wide range of concentrations is described. Traceability to SI units is achieved by comparing the CPC to an AE at high concentrations, fixing the constant of proportionality. The result is a CPC calibrated with traceability to SI units and uncertainties assigned to concentrations from 1 particle·cm<sup>-3</sup> to 10<sup>4</sup> particles·cm<sup>-3</sup>.

## INTRODUCTION

A condensation particle counter (CPC) is expected to have a proportional response at low concentrations, where particles pass through the detection volume with enough spacing in time so that a second particle appearing while the first is being counted is very unlikely. Still it is important to verify this proportional response experimentally. Specifically, this is important to the military as the CPC is used by the military for verifying the ability of the Joint Service Mask Leakage Tester (JSMLT) to measure the leakage of a test aerosol into military-issue gas masks over 4 orders of magnitude. Another application of CPC counting over 4 orders of magnitude is the counting of macromolecules (Lewis et al., 1994). There have also been a number of recent studies on CPC performance motivated by legislated vehicle number emission measurements. These studies have focused on the effects of particle size, particle type, and concentration on the CPC performance (Giechaskiel et al., 2009; Wang et al, 2010). The linearity testing of the CPC versus concentration in these studies have been for concentrations larger than 1000 particles·cm<sup>-3</sup> for which the aerosol electrometer is a traceable measurement.

The focus of this study is to verify proportional counting over the concentration range from 1 particle·cm<sup>-3</sup> to 10<sup>4</sup> particles·cm<sup>-3</sup>. Another goal of the research is to obtain a traceable proportionality constant by comparison of the CPC response at high concentrations to the aerosol electrometer measurements performed at NIST (Fletcher, 2009).

Several approaches to verifying the CPC response at low concentrations were considered, all involving diluters. Initially, the development of a traceable diluter capable of diluting by as much

as  $10^4$  was considered. Brockmann et al. (1984) developed an extraction diluter and Hueglin et al. (1997) a rotating cavity diluter both with the ability to dilute by four orders of magnitude. However, these dilution measurements were not traceable measurements. A traceable measurement would require an accurate measurement of diluter flow rates and of the particle losses through the diluter. The second approach considered involves using two CPCs calibrated with the aerosol electrometer (AE) from about  $(10^3 \text{ to } 10^4)$  particle·cm<sup>-3</sup> to calibrate an adjustable diluter for a factor of about 10. The diluter is then used to dilute down from the lowest CPC concentration calibrated by the AE. Next the diluter is adjusted to give a factor of about 100, using the highest CPC calibration point and the previously diluted low concentration. This process is continued until the lowest desired CPC concentration is calibrated. While the diluter used in this scheme is simple and inexpensive, the data analysis is quite involved when multiple dilutions are performed and the uncertainty increases with each successive dilution.

The third approach, which is the focus of this study, is analogous to the method for testing the linearity of high power laser detectors (Li et al., 2004). The linearity test of the laser detector uses a rotating optical chopper as a consistent attenuator. The detector output voltage is measured with and without the attenuator as the laser power is varied from 1 W to about 1000 W. In our case a consistent diluter serves the role of the attenuator. The diluter is adjusted at low concentrations to give a fixed dilution ratio of about 10, measured by two CPCs. The measurement of this fixed dilution ratio at multiple concentrations between 1 particle·cm<sup>-3</sup> to  $10^4$  particles·cm<sup>-3</sup> is used as a proportionality test of the CPC response, based on the fact that for a truly proportional CPC the dilution ratio will be independent of the challenge concentration.

As the concentration is raised, the effect of coincidence counting becomes a source of non-linearity. Typically an iterative or dead-time coincidence correction is made to the CPC measurements to reduce the non-linear effect and restore the CPC to a linear response. This study will assess the ability of the coincidence correction to preserve a proportional response up to a concentration of  $10^4$  particles·cm<sup>-3</sup>.

Measurements of the diluter pressures and temperature are made to determine the constancy of the diluter over time. Once the CPC is verified to be proportional, the coefficient of proportionality is measured by comparison with an AE at high concentration. This comparison results in an absolute calibration of the CPC and provides traceability to SI units through the NIST realizations of the volt and the amp. This approach takes advantage of the capabilities of the AE, using it only at the highest concentrations that the CPC can measure, so that measurement uncertainty of the CPC calibration can be reduced.

In an effort to make the measurements as accurately as possible (JCGM, 2008; 2.13-2.15), the uncertainties associated with the flow measurement of the CPC and the sampling bias when comparing two CPCs was reduced to less than 1 %. This study goes beyond current CPC calibration studies in this regard and the methodology and the results are presented in Appendices A and B.

This report proceeds by describing the aerosol generator and the measurement process for the CPC calibration. The accuracy of the proportional model is determined by calibrating the CPC flow rates, performing a direct comparison between two CPCs, and then using the CPCs to measure a dilution factor over a range of concentrations. The CPC is then compared to an AE. Finally the measurement uncertainty is described and conclusions are drawn.

## AEROSOL GENERATOR

The aerosol generator is designed to produce a monodisperse oil aerosol of 100 nm particles in dry air, with a stable and adjustable concentration from 1 particle·cm<sup>-3</sup> to 10<sup>4</sup> particles·cm<sup>-3</sup>. As shown in Figure 1 a Collision atomizer (3076 Constant Output Atomizer, TSI, Inc.)<sup>1</sup> is used to spray a dilute solution of approximately 0.5 mL emery oil in 1 L of reagent grade isopropanol alcohol, resulting in a peak in the atomized size distribution that is less than 100 nm. The emery oil is a branched polyalphaolefin (1-decene tetramer mixed with 1-decene trimer, hydrogenated; also identified as PAO 4 cSt). The aerosol flows through a bi-polar charger (Kr-85 source, 3077, TSI, Inc.) at about 3 L/min, a single stage micro orifice uniform deposition impactor (MOUDI) (MSP Corp) with a pressure drop of about 17 kPa, and then to a 2 L accumulator, where the aerosol is vented through a filter to the atmosphere. The polydisperse aerosol in the accumulator is drawn by the CPCs through two diluters in series, a flow meter, a second bi-polar charger, a differential mobility analyzer (DMA) (3081 Long DMA, TSI, Inc), and then into the particle detectors.

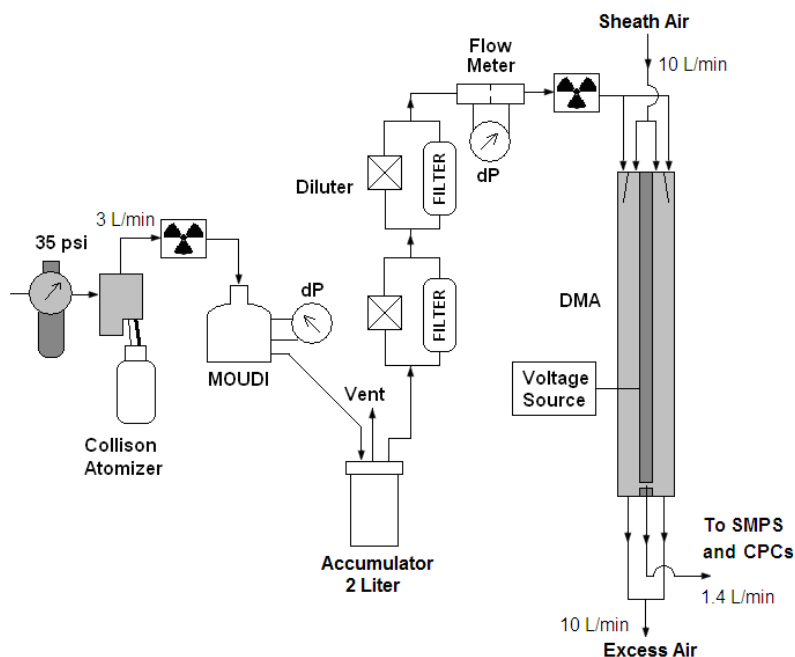


Fig. 1. Aerosol source schematic

To reduce the number of larger particles that can pass through the DMA with multiple charges, two modifications were made. First, the oil-alcohol solution was mixed so that the peak in the polydisperse number concentration was lower than the 100 nm target diameter. Thus the target diameter resides in the long tail of the polydisperse size distribution. Second, a MOUDI was positioned just downstream of the Collision atomizer to produce a sharp cut-off of the polydisperse size distribution. A nominal cut point of 125 nm at 2 L/min was used; however, the

<sup>1</sup> Certain commercial equipment, instruments, or materials are identified in this paper in order to specify the experimental procedure adequately. Such identification is not intended to imply recommendation or endorsement by the National Institute of Standards and Technology, nor is it intended to imply that the materials or equipment identified are necessarily the best available for the purpose.

full aerosol flow rate of 3 L/min was passed through the MOUDI, producing a lower cut point of about 115 nm. The result of these two modifications was a monodisperse 100 nm aerosol with about 0.3% of double charged particles exiting the DMA, and the effective elimination of triple charged particles.

Prior to reaching the DMA, the aerosol concentration was stabilized by using a 2 L accumulator to dampen fluctuations in the generator. The concentration was controlled by adjusting two diluters in series downstream of the accumulator. The DMA was operated at 10 L/min sheath flow rate in non-recirculating mode. By dumping the excess flow and not recirculating it as sheath flow, the isopropanol vapor present in the incoming aerosol is confined to the edge of the DMA and does not exit in the monodisperse aerosol flow. Thus the carrier gas for the calibration aerosol is simply dry filtered air.

## DILUTION MEASUREMENT

### Overview

To validate the proportional model for the CPC, two CPCs and an adjustable diluter are used. All measurements of concentration by the CPCs are corrected for coincidence by iterating equation 1 for  $i=1, \dots, 4$  by which time the result had converged for all concentrations within the scope of this application:

$$C_{C_i} = \frac{N}{tQ_v} \exp C_{C_{i-1}} Q_v \tau, \text{ for } i=1, \dots, 4 \text{ with } C_{C_0} = C_{\text{Observed}} = \frac{N}{tQ_v}. \quad (1)$$

In equation 1  $C_{C_4}$  is the coincidence corrected concentration [particles·cm<sup>-3</sup>],  $N$  is the number of pulses recorded by the CPC,  $t$  is the sample time [s],  $Q_v$  is the volumetric flow rate [cm<sup>3</sup>·s<sup>-1</sup>], and  $\tau$  is the recovery time of the electronics between successive count events,  $\tau$ , which includes the transit time (particle in the intense region of the light source) and the stretch time (pulse processing time of the multichannel analyzer) (taken as 0.4  $\mu$ s). A schematic of the dilution assembly is shown in Figure 2. The undiluted aerosol concentration is measured by CPC 2 and the diluted concentration by CPC 1. The pressure drop across the diluter is monitored by the inlet pressure of each CPC. The valve is used to adjust the dilution factor by changing the relative amount of aerosol that flows through the orifice and HEPA filter. A key attribute of the diluter is that the dilution factor is independent of the aerosol concentration. This is a result of the flows through the diluter orifice and the CPC critical orifice being insensitive to aerosol concentrations of 100 nm monodisperse emery oil droplets up to number concentrations of at least 13000 particles·cm<sup>-3</sup>. It is shown in Appendix A that the CPC inlet flow rate is insensitive to the presence of the monodisperse aerosol. The flow through the diluter orifice was also measured at high and low concentrations, with the results shown in Table 1.

Table 1  
The effect of aerosol on the diluter orifice flow rate.

Concentration $\text{cm}^{-3}$	Flow Rate $\text{cm}^3/\text{min}$	$P_{\text{up}}$ kPa	$P_{\text{down}}$ kPa
12200	138.5	98.02	97.30
0	137.8	98.01	97.29
13000	138.1	98.00	97.28
0	137.8	97.99	97.27
13700	138.7	97.98	97.26
0	139.2	97.98	97.26

The ratio of the high and low concentration flows is within 0.5% of unity for all three measurement sequences. This value is equal to the standard uncertainty of the volume displacement flow meter (BIOS 510-L, Bios, Inc.) and is considered a negligible effect. The ability of the mixing orifice to produce a well mixed aerosol was verified in a study of sampling bias described in Appendix B. It was found that the effect of sampling bias from the mixing and the sampling lines was at most 0.04 %.

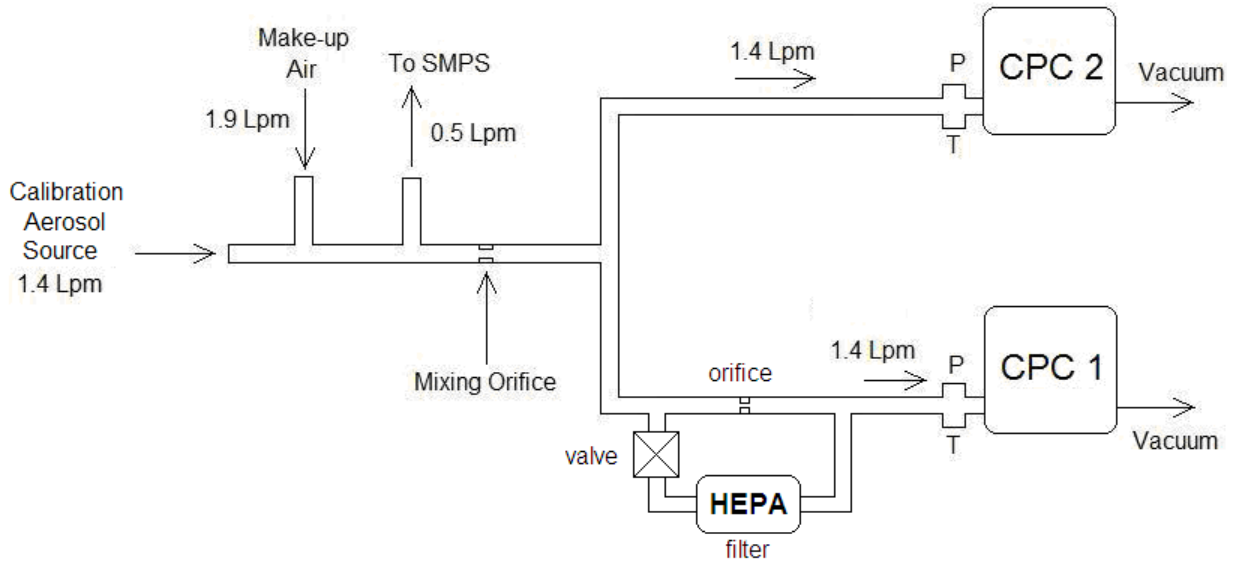


Fig. 2. Aerosol dilution assembly schematic

Before making dilution factor measurements, a direct comparison calibration of the two CPCs is performed by challenging both CPCs with the same aerosol source and comparing concentrations. This calibration accounts for slight differences between the two instruments that could effect the dilution measurements. Next dilution measurements are performed using the setup in Figure 2. The diluter is adjusted to give a ratio of about 0.10 between the low concentration in CPC1 and the high concentration in CPC2, which is set to about 100 particles- $\text{cm}^{-3}$ . The high concentration is then adjusted to several different test points. The sequence of the concentration test points is randomly selected, and the initial test point used to

set the dilution ratio is repeated at the end of the sequence. One example of test sequences that could be used to measure the constancy of the dilution factor is ( $10^2$ ,  $3 \times 10^3$ ,  $10^4$ ,  $10^2$ ,  $10^3$ ,  $3 \times 10^2$ , 30, 10, and  $10^2$ ) particles·cm<sup>-3</sup>. The dilution factor is computed at each concentration as the ratio of the two CPC measurements multiplied by the appropriate correction factor from the direct comparison of the CPCs.

### Direct Comparison

The direct comparison measurement is required to account for any differences between the two detectors when measuring the dilution factor. The direct comparison process consists of two steps: calibration of the CPC inlet flow rates and the comparison of concentration measurements made simultaneously by both CPCs.

The inlet volumetric flow rate of each CPC is controlled by a critical orifice. It is known that the CPC inlet volumetric flow rate is independent of pressure and is a weak function of temperature when controlled with a critical orifice. Thus a single flow calibration prior to performing concentration measurements is sufficient, given that the temperature does not change by more than 1 °C. As presented in Appendix A, the within day random uncertainty was about 0.07%, the day to day variability about 0.3 %, and the standard uncertainty in the traceable flow calibration instrument, a volume displacement flow meter (Bios Defender 510-M, Bios, Inc.), is 0.5% of reading. After the flow calibration, the direct comparison is performed. This measurement was accomplished by splitting the flow from the aerosol source to both CPCs simultaneously. Accurate measurement of the flow splitter bias was performed and is detailed in Appendix B, which shows that the aerosol is well mixed and that no correction is needed for the direct comparison analysis. Measurements of concentration are made at the seven test points of ( $10^4$ ,  $3 \times 10^3$ ,  $10^3$ ,  $3 \times 10^2$ ,  $10^2$ , 30, and 10) particles·cm<sup>-3</sup>. The ratio of concentration measured by CPC 1 to CPC 2 is computed for each concentration; for example, the ratio for CPC 1=10 particles·cm<sup>-3</sup> and CPC 2=10.1 particles·cm<sup>-3</sup> is given by

$$k = C_1 / C_2 = 10 / 10.1 \quad (2)$$

As discussed below, this constant is used to correct the reading of the undiluted aerosol,  $C_2$ , to predict the undiluted reading for  $C_1$ .

### Dilution Measurements

The dilution factor is measured using the setup in Figure 2. The diluter was first adjusted to give a factor of about 0.1. The concentrations were then varied according to a randomized sequence of the prescribed seven test points. The CPC inlet temperatures were within +/- 0.1°C and the CPC inlet pressures were held constant within +/- 0.1% over the one hour period for dilution measurements for a single day. The constancy of the inlet pressure and temperature are essential to minimize the drift in the dilution factor. The dilution factor is computed by equation 3, where the concentration of the diluted aerosol, measured by CPC 1, is in the numerator:

$$R_D = \frac{C_1}{k(C_2)C_2} \quad (3)$$

All concentrations were computed using ten second sample intervals for a total collection time of two minutes, except for the highest concentration which was collected for one minute, to reduce

the uncertainty due to Poisson counting errors. The coincidence correction from equation (1) was iterated four times to obtain sufficient convergence at high concentrations. The data for a single day's measurement are shown in Table 2, which shows the diluted and undiluted concentrations, the correction factor  $k$ , the average dilution factor, and standard deviation of the mean for each measurement. The average dilution factor for each measurement is computed as

$$\overline{R_D} = \frac{1}{n} \sum_{k=1}^n R_{D,k} \quad , \quad (4)$$

and the standard deviation of the mean is

$$S_{R_D} = \sqrt{\frac{1}{n-1} \sum_{k=1}^n (R_{D,k} - \overline{R_D})^2} \quad . \quad (5)$$

Table 2  
Dilution factor measurements for a single day

test	CPC1	CPC2	k(CPC2)	$\overline{R_D}$	$S_{R_D}$
1	1.080E+01	1.046E+02	0.976	0.1058	6.9E-04
2	1.024E+02	9.936E+02	0.980	0.1052	2.0E-04
3	1.016E+00	9.696E+00	0.978	0.1071	2.0E-03
4	1.385E+03	1.338E+04	0.971	0.1066	6.5E-05
5	3.121E+01	3.043E+02	0.976	0.1051	4.9E-04
6	1.108E+01	1.073E+02	0.976	0.1058	6.8E-04
7	3.448E+00	3.373E+01	0.980	0.1043	5.3E-04
8	3.076E+02	2.965E+03	0.977	0.1062	1.6E-04
9	1.084E+01	1.048E+02	0.976	0.1060	4.6E-04

It is seen from Table 2 that the value of  $S_{R_D}$  decreases about 30 fold from a value of  $2.0 \times 10^{-3}$  to less than  $1 \times 10^{-4}$  as the CPC 1 concentration increases from 1 particle·cm<sup>-3</sup> to  $1.4 \times 10^3$  particles·cm<sup>-3</sup> as a result of the Poisson counting statistics for the CPC. Figure 3 shows graphically that the dilution ratio is nearly constant over a wide range of concentrations with a narrow range of values for each day. However, the range of values is not as narrow as expected at concentrations of 100 particles·cm<sup>-3</sup> and larger based on the values of  $S_{R_D}$ . The larger uncertainty is a result of a slight drift in one of the CPC flows or a slight drift in the diluter. To assess the significance of the drift, the data were replotted as a function of measurement number which is roughly proportional to time. A total of nine dilution measurements were made on each day. The data are shown along with linear best fits to each data set. The fact that the slopes of these lines are nearly zero, and no other clear systematic variation is visible in the data, indicates that there is no significant drift in the dilution ratios throughout the day. A standard statistical test based on the t – distribution also supports this conclusion. The T-statistics for the test of the slope each day versus a hypothesized value of zero were observed to be T = -1.56, T = -0.35, and T = 0.93. The fact that the absolute values of the T-statistic are smaller than the critical value, t(95%) = 2.36 based on seven degrees of freedom, indicates that none of these slopes are significantly different than zero.

Table 3 shows the average and the relative standard deviation of the mean for each day's repeat measurements of  $\overline{R_D}$ , denoted by  $\overline{\overline{R_D}}$  and  $S_{\overline{R_D}}/\overline{\overline{R_D}}$ , respectively. Equations 4 and 5 were used to compute these values for each day by replacing  $R_D$ ,  $\overline{R_D}$ , and  $S_{R_D}$  with  $\overline{R_D}$ ,  $\overline{\overline{R_D}}$ , and  $S_{\overline{R_D}}$ , respectively. These values give an estimate of the constancy of the dilution factor over a range of concentrations. The square root of the average of the three relative variances, with a value of 0.0022 corresponding to 0.22%, is used as the typical standard uncertainty associated with the dilution testing.

Table 3  
The average dilution factor and relative standard deviation of the mean for three different days

Test Day	$\overline{\overline{R_D}}$	$S_{\overline{R_D}}/\overline{\overline{R_D}}$
1	0.0941	0.0021
2	0.1058	0.0027
3	0.1070	0.0017

The data given in Tables 2 and 3 indicate that the proportional model for the CPC is valid over this concentration range when used with the specified sample times and coincidence correction. Figure 3 shows that there is no concentration dependent bias of the dilution factor measurement and Figure 4 shows that there is no bias from drift in this data. This also verifies that the coincidence correction factor accurately accounts for coincidence effects for concentrations up to 13000 particles·cm<sup>-3</sup>.

Finally, Figure 5 compares the concentrations computed with and without the coincidence correction using equation 3 for a single day of measurements. At concentrations below 1000 cm<sup>-3</sup> the dilution factors are nearly identical. As the concentration increases above 1000 particles·cm<sup>-3</sup> the dilution factors for the data with no coincidence corrections applied increase, revealing a non-linearity in the CPC. The increase in dilution factor is due to the undercounting of the high concentration, caused by coincidence. This graph indicates that the dilution process described in this paper is capable of detecting a non-linearity in the CPC response.

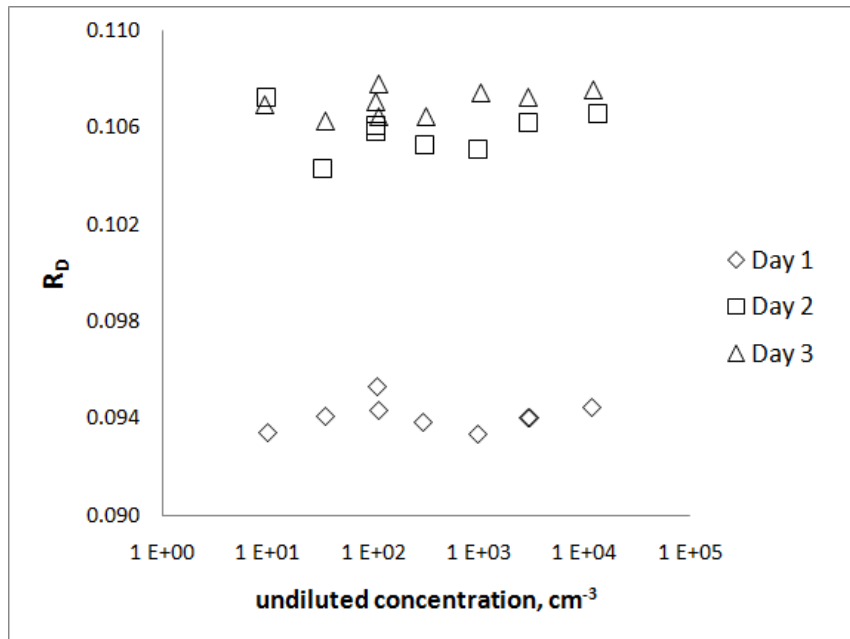


Fig. 3. Graph of all measured dilution factors versus undiluted concentration.

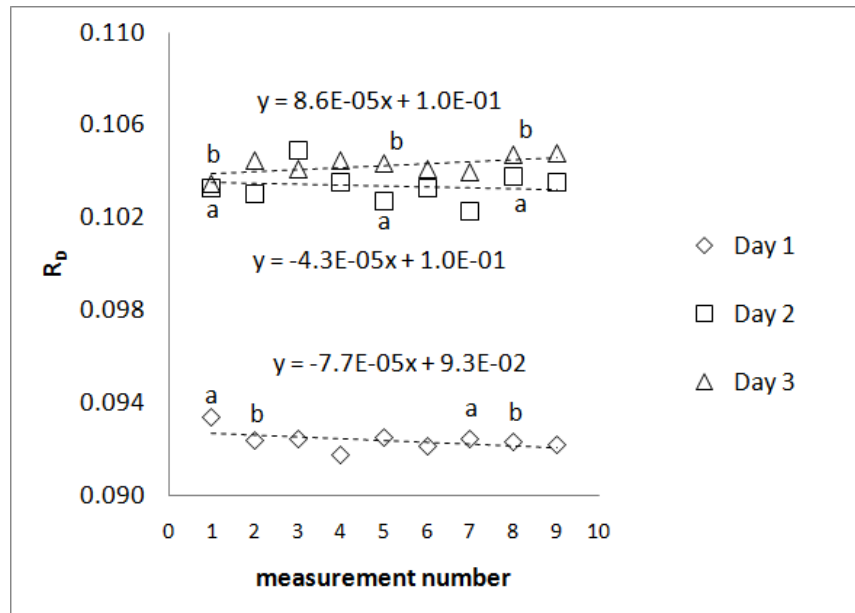


Fig. 4. The dilution ratio is plotted versus the time ordered test number for the data collected on each of the three days. The letters next to the symbols indicate points where repeat measurements were made for nominally identical undiluted particle concentrations. The dashed lines are least-squares regression lines assuming linear drift.

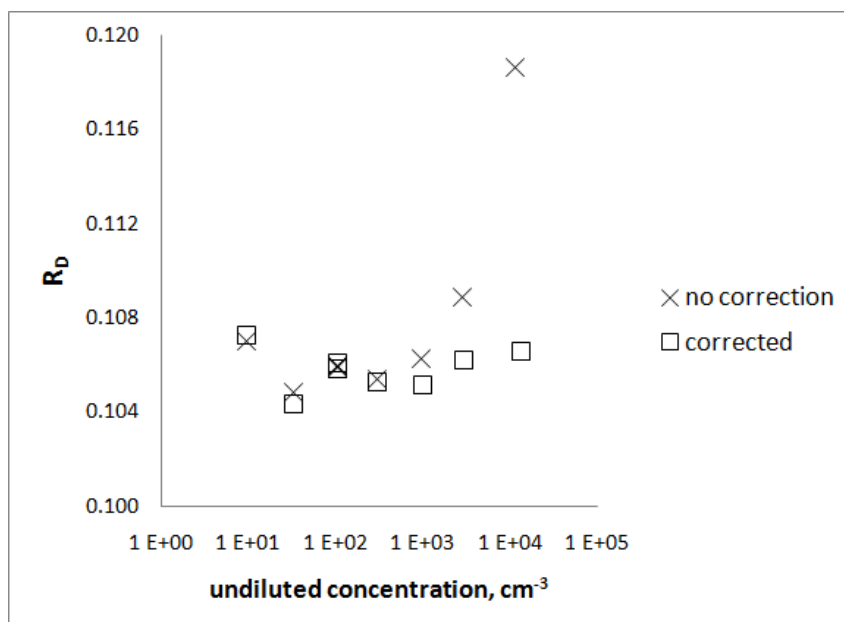


Fig. 5. Dilution factors for day two data with and without coincidence correction.

## PRIMARY CALIBRATION

A NIST traceable calibration of a condensation particle counter (CPC) using an aerosol electrometer was carried out for the Army Primary Standards Laboratory (Fletcher, 2009) over the concentration range from about (300 to 13000) particles·cm<sup>-3</sup>. A subsequent reanalysis of the data and the inclusion of a flow effect resulting from the presence of CO<sub>2</sub> in the air flow has been submitted for publication by Mulholland et al. (2010). We make use of this revised calibration data for establishing a traceable CPC over the concentration range from (1 to 13000) particles·cm<sup>-3</sup>. The successive dilution experiments have established the linearity of the CPC over this concentration range. The traceable calibration is needed to obtain an accurate proportionality constant for the relationship between the CPC concentration and the NIST traceable concentration, N<sub>AE</sub>. To determine the proportionality constant, we compute the ratio of N<sub>AE</sub> to N<sub>CPC</sub> for the six sets of data at the largest concentrations in the range from about 9500 particle·cm<sup>-3</sup> to almost 13000 particles·cm<sup>-3</sup> (Mulholland et al., 2010, Table 1). The largest concentrations are used to minimize the effect of a possible systematic bias in the aerosol electrometer at low concentrations. The mean value of the proportionality constant, C<sub>pro</sub>, and the standard deviation of the mean are: 1.0236 ± 0.0032. The mean value of the proportionality constant based on these six points is 0.28 % larger than the proportionality constant based on all the data points and is within one standard uncertainty of the mean value based on all the points.

A major component in the uncertainty of this proportionality constant is the uncertainty in both the aerosol electrometer flow and the CPC flow resulting from the presence of CO<sub>2</sub> in the flows. As described in Mulholland et al. (2010), the resulting relative standard uncertainty in traceable CPC concentration is 1.10 %. The standard uncertainty in the proportionality constant,  $u_1(C_{pro})$ , resulting from both effects, is computed as the root-sum-of-squares (RSS) of the standard deviation of the mean of C<sub>pro</sub> and the standard uncertainty of the CO<sub>2</sub> effect on flow and has a final value of  $u_1(C_{pro}) = 0.0117$ .

The last component of uncertainty is the constancy of the proportionality constant, which was computed to be 0.0022. The propagation of this uncertainty value with  $u_1(C_{pro})$  results in a

combined standard uncertainty of  $u_c(C_{\text{pro}}) = 0.012$ . The corresponding expanded uncertainty is  $U = 0.024$  computed using a coverage factor of  $k = 2$ .

The concentrations measured in the primary calibration were computed with a standard volumetric flow rate referenced to 101325 Pa and 25 °C. Equation 6 can be used to convert concentrations calculated with the actual volumetric flow rate to a concentration referenced to standard conditions.

$$C_{\text{ref}} = C \frac{P_{\text{ref}}}{P} \frac{T}{T_{\text{ref}}} \quad (6)$$

In equation 6,  $C$ ,  $P$ , and  $T$  are the actual concentration, pressure, and temperature, while  $C_{\text{ref}}$ ,  $P_{\text{ref}}$ , and  $T_{\text{ref}}$  are the reference concentration, pressure, and temperature.

## CONCLUSIONS

In this study we have used a fixed diluter to verify the proportionality of a CPC from 1 particle·cm<sup>-3</sup> to 10<sup>4</sup> particles·cm<sup>-3</sup>. The stability of the diluter over time was verified by monitoring the differential pressure across the diluter and the temperature at the inlets of the CPCs, along with comparison of repeated measurements of the dilution factor at the same concentration throughout the calibration. There was no concentration dependent bias observed in the dilution factor over three days of testing. By comparing the CPC to an AE at high concentrations to fix the constant of proportionality, an absolute calibration of the CPC traceable to SI units is accomplished with a relative expanded uncertainty of 2.4%. A thorough analysis of the CPC inlet flow calibration is given in the Appendix A along with a method to measure the bias that results from splitting an aerosol flow between two detectors. These calibrations enable the CPC to perform accurate measurements of concentration with an uncertainty about 1000 times lower than was previously possible with the AE calibration alone, and provides a solution for laboratories that require traceable calibration of CPCs at low concentrations. The authors believe that this is an economical and analytically simple approach to calibrating a CPC at low concentrations, as well as providing an accurate estimate of the uncertainty.

## REFERENCES

- Brockman, J. G., Lui, B.Y.H. and McMurry, P.H. (1984) A Sample Extraction Diluter for Ultrafine Aerosol Sampling, *Aerosol Sci Technol.*, **3** (4), 441-451.
- Fletcher, R.A., Mulholland, G.W., Winchester, M.R., King, R.L., and Klinedinst, D.B. (2009). Calibration of a Condensation Particle Counter Using a NIST Traceable Method, *Aerosol Science and Technology*, 43:425–441.
- Giechaskiel, B., Wang, X., Horn, H.- G., Spielvogel, J., Gerhart, C., Southgate, J., Jing, L., Kasper, M., Drossinos, Y., and Krasenbrink, A. (2010). Calibration of Condensation Particle Counters for Legislated Vehicle Number Emission Measurements, *Aerosol Science and Technology*, 43:1164 - 1173.

Hueglin, Ch., Scherrer, L., and Burtscher, H. (1997) An Accurate, Continuously Adjustable Dilution System (1:10 to 1:10<sup>4</sup>) for Submicron Aerosols, *J. Aerosol Sci.*, **28**, 1049-1055.

Joint Committee on Guides in Metrology (JCGM) International Vocabulary of Metrology – Basic and general concepts and associated terms (VIM), 2008, <http://bipm.org/en/publications/guides/vim.html>.

Kenneth C. Lewis, C, Dohmeier, D., Jorgenson, J., Kaufman, S., Zarrin F., and Dorman, F. (1994) Electrospray-Condensation Particle Counter: A Molecule-Counting LC Detector for Macromolecules, *J. Analytical chemistry* **66**, 2285-2292.

Li, X., Scott, T., Yang, S., Cromer, C., and Dowell, M. (2004) Nonlinearity Measurements of High-Power Laser Detectors at NIST, *J. Res. Natl. Inst. Stand. Technol.* **109**, 429-434.

Mulholland, G.W, Guthrie, W.F., and Fletcher, R.A., (2010) Revised Calibration of a Condensation Particle Counter Using a NIST Traceable Method, submitted to *Aerosol Science and Technology*.

Taylor, B. N., and Kuyatt, C. E. (1994). Guidelines for Evaluating and Expressing the Uncertainty of the NIST Measurement Results. NIST Technical Note 1297. U.S. Government Printing Office, Washington, DC.

Wang, X., Caldow, R., Sem, G.J., Hama, N. and Sakurai, H. (2010) Evaluation of a Condensation Particle Counter for Vehicle Emission Measurement: Experimental Procedure and Effects of Calibration Aerosol Material. *J. Aerosol Sci.*, **41** (3), 2010, pp. 306-318.

## APPENDIX A: CPC FLOW CALIBRATION

The CPCs in this study use critical orifices that control the mass flow rate by Eq. (4) (Miller, 1983) as

$$q_m = C_d A_t C_* \frac{P_o}{\sqrt{\frac{R}{mw} T_o}} \quad . \quad (A1)$$

The CPC inlet volumetric flow rate is derived by dividing the mass flow rate by the fluid density for an ideal gas,

$$Q_v = \frac{q_m}{\rho} = C_d A_t C_* \frac{P_o}{P} \frac{T}{\sqrt{T_o}} \sqrt{\frac{R}{mw}} \quad . \quad (A2)$$

In Eq. A1 and A2,  $q_m$  is the mass flow rate,  $Q_v$  is the volumetric flow rate,  $C_d$  is the discharge coefficient,  $A_t$  is the orifice area,  $C_*$  is the compressibility factor,  $P_o$  and  $T_o$  are the stagnation pressure and temperature,  $P$  and  $T$  are the static pressure and temperature,  $mw$  is the relative molecular mass, and  $R$  is the universal gas constant. The ratios of static to stagnation pressure and temperature for isentropic flow are

$$\frac{P_o}{P} = \left( 1 + \frac{\gamma - 1}{2} M^2 \right)^{\frac{\gamma}{\gamma - 1}} \quad (A3)$$

$$\frac{T_0}{T} = 1 + \frac{\gamma - 1}{2} M^2 \quad , \quad (A4)$$

where  $M$  is the Mach number and  $\gamma$  is the ratio of specific heats, taken to be 1.4. An estimate for flow velocity of 0.8 m/s is obtained by dividing the volumetric flow rate of 1.5 L/min by the area of a circular pipe of 0.64 cm (0.25 inch) diameter. For a gas temperature of 25 °C the sound speed in air is 346 m/s, and the pressure and temperature ratios are 1.000004 and 1.000001, respectively. Thus, considering that the static and stagnation pressures and temperatures at the inlet of the CPC are equivalent, equation A2 simplifies to

$$Q_v = C_d A_t C_* \sqrt{\frac{R}{M} T} \quad . \quad (A5)$$

Equation A5 shows that the CPC inlet volumetric flow rate is independent of pressure and a weak function of temperature and the fluid relative molecular mass.

To test the relationships in Equations 4 and 5, a piston-displacement volumetric flow meter (Bios Defender 510-M, Bios, Inc.) was used to measure the inlet volumetric flow rate with a relative standard uncertainty of 0.5 %. The inlet static pressure and temperature were measured to convert volumetric to mass flow rate. The measured volumetric flow rate was converted to the inlet volumetric flow rate by correcting for fluid density changes across the meter. All measurements were made with the CPCs powered on and filled with butanol, using air dried to a relative humidity of approximately 15 %. The CPC inlet volumetric and mass flow rates were measured on one day over a range of inlet pressures and at constant inlet temperature (within 0.5 °C). The flow rate measurements are shown in Figures A1 and A2, revealing the linear dependence of mass flow rate and the constancy of the inlet volumetric flow rate for a range of inlet pressures, as predicted by Equations A1 and A2. The uncertainty bars shown in each plot are expanded uncertainties based on a coverage factor of  $k = 2$ .

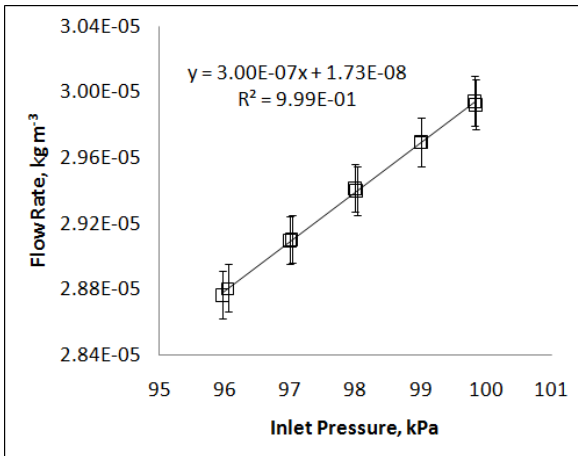


Figure A1: CPC inlet mass flow rate.

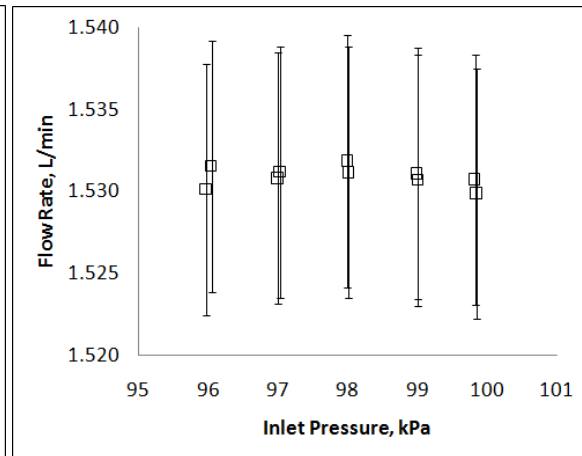


Figure A2: CPC inlet volumetric flow rate.

The one day mean for the discharge coefficient and inlet volumetric flow rate over the range of pressures are 0.800 L/min (13.33 cm<sup>3</sup>s<sup>-1</sup>) and 1.461 L/min (24.35 cm<sup>3</sup>s<sup>-1</sup>), respectively. The relative standard deviation is 0.0007 for both cases. As expected, the discharge coefficient is effectively constant over this range of pressures, and consequently, by Eq. A2, the volumetric flow rate is also constant. Three different days of inlet volumetric flow rate measurements are shown in Figure A3.

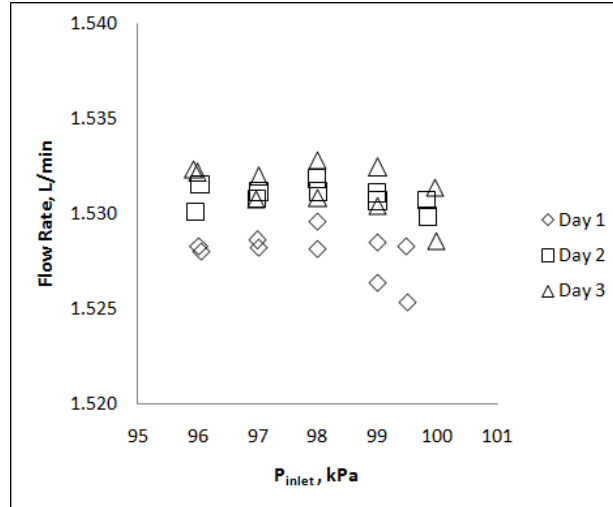


Figure A3: CPC inlet volumetric flow rate for 3 days.

The three day relative standard deviation for the discharge coefficient and volumetric flow rate are 0.0028 and 0.0025, respectively. While systematic differences are observed from day to day, the variation over three days is within the experimental uncertainty expected from the flow standard.

The dependence of the CPC inlet flow rate on aerosol concentration was also estimated using the same volume displacement flow meter. This meter should be insensitive to aerosol concentration, provided that the concentration is not high enough to coat the interior of the piston cylinder and cause it to stick. A baseline volumetric flow rate was measured with particle free air, and then the concentration was raised incrementally to approximately  $10^4$  particles·cm<sup>-3</sup> using 100 nm emery oil droplets. Table A1 shows that the flow rate controlled by the critical orifice is insensitive to the presence of the aerosol at the concentrations tested. Therefore, the effect of aerosol on the inlet volumetric flow rate was ignored.

Table A.1: Effect of aerosol concentration on the CPC inlet volumetric flow rate

Concentration [cm <sup>-3</sup> ]	Flow Rate [cm <sup>3</sup> /s]	Flow Rate [L/min]
0	24.73	1.484
30	24.75	1.485
350	24.73	1.484
450	24.73	1.484
1690	24.75	1.485
6260	24.72	1.483
9800	24.72	1.483

The CPC inlet pressure and temperature are recorded to allow the conversion between the actual inlet volumetric flow rate and the standard volumetric flow rate referenced to 25 °C and 101325 Pa (STP). It is noted that while the actual volumetric flow rate is independent of pressure, the volumetric flow rate referenced to STP is essentially a scaled mass flow rate, and is therefore linearly dependent on the inlet pressure.

## APPENDIX B: AEROSOL SPLITTER BIAS MEASUREMENT

The objective of the aerosol mixer and splitter assembly is to simultaneously challenge both CPCs with equal aerosol concentrations. Any bias introduced by the aerosol mixer and splitter assembly will result in each CPC being challenged with a different aerosol concentration. Unless the bias is measured and properly corrected for, an error will be introduced into the calibration.

To derive the equation used to quantify the aerosol splitter bias, consider a monodisperse aerosol source that is connected to a mixer and flow splitter, where the mixer is imperfect and the splitting produces a bias, shown in Figure B1.

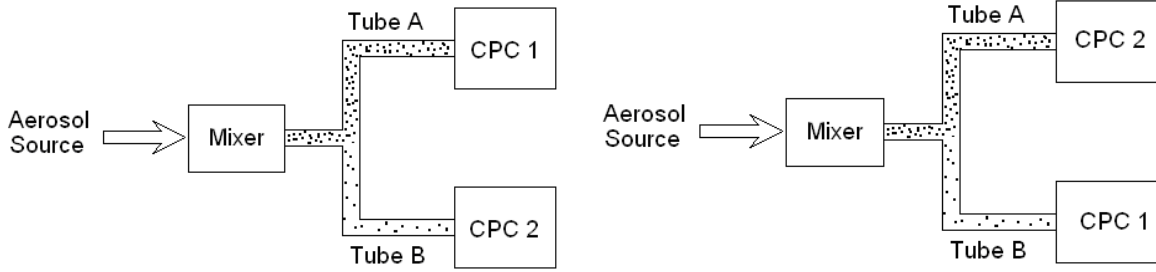


Figure B1: Aerosol splitter schematic with concentration bias for two CPC configurations.

Figure B1 shows that the CPC connected to Tube A is challenged with a higher concentration than the CPC connected to Tube B. The splitter bias is defined with respect to the mixer and splitter tube orientation as

$$\beta \equiv C_A / C_B , \quad (\text{B1})$$

Where  $\beta$  is the splitter bias correction factor, and  $C_A$  and  $C_B$  are the aerosol concentrations at the inlet of the CPCs connected to tubes A and B, respectively. Note that the splitter bias correction factor  $\beta$  is configuration dependent because it is defined with respect to the mixer, splitter, and connective tubing orientation. Thus, the concentration measured by the CPC connected to Tube B must be multiplied by the correction factor  $\beta$  to account for the bias. For the configuration in Figure B1, we have

$$\beta_I \equiv \frac{C_A}{C_B} = \left( \frac{\eta_1 C_1}{\eta_2 C_2} \right)_I \quad (\text{B2})$$

Where  $C_1$  and  $C_2$  are the measured aerosol particle concentrations by the CPC 1 and CPC 2, and  $\eta_1$  and  $\eta_2$  are calibration factors for CPC 1 and CPC 2. For a monodisperse test aerosol these calibration factors depend on the aerosol concentration and the particle diameter. Exchanging the CPCs as shown in Figure B1 gives

$$\beta_{II} \equiv \frac{C_A}{C_B} = \left( \frac{\eta_2 C_2}{\eta_1 C_1} \right)_{II} . \quad (\text{B3})$$

Exchanging the two CPCs is equivalent to flipping the mixer and splitter, as long as the mixer and splitter provide the same bias when flipped. For equal CPC flow rates, the bias given by equations (B2) and (B3) are equal. By multiplying equations (B2) and (B3) and making use of the equality of the  $\beta$ 's, we obtain

$$\beta = \sqrt{\frac{\epsilon_2 C_2}{\eta_1 C_1} / \frac{\epsilon_1 C_2}{\eta_1 C_1}} \quad , \quad (B4)$$

If the measurements are performed at the same concentrations and particle size, the CPC calibration factors cancel and the bias correction factor can be measured with un-calibrated CPCs.

$$\beta = \sqrt{\frac{\epsilon_2}{\eta_1} / \frac{\epsilon_1}{\eta_1}} = \sqrt{r_{II} / r_I} \quad (B5)$$

$$r = C_2 / C_1 \quad (B6)$$

The assembly used to challenge two CPCs with the calibration aerosol source is shown in Figure 3. The aerosol flows in from the source at 1.4 L/min, while the two CPCs and a scanning mobility particle sizer (SMPS) sample the calibration aerosol at a total combined flow rate of 3.3 L/min. To maintain flow, 1.9 L/min of dry filtered make-up air is introduced to the system. The aerosol was mixed using a 0.241 cm (0.095”) diameter orifice in a 0.46 cm (0.18”) inner diameter tube. The two branches of the aerosol splitter that connect to each CPC are nearly equivalent in geometry, and both are rigid stainless steel tubing.

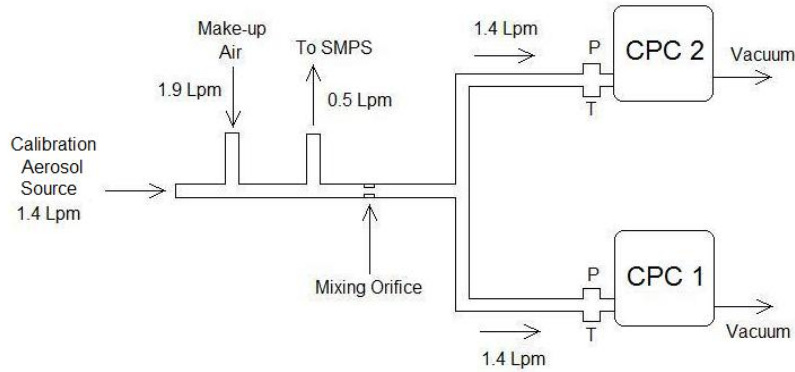


Figure B2: Schematic of aerosol mixer, splitter, and upstream plumbing.

The flow splitter bias correction factor  $\beta$  was computed using equation B5 by measuring the concentration with both CPCs as shown in Figure B1. The procedure was carried out fifteen times over two consecutive days. The data is plotted in Figure B3, where the error bars represent the standard uncertainty of the flow splitter correction factor  $\beta$ .

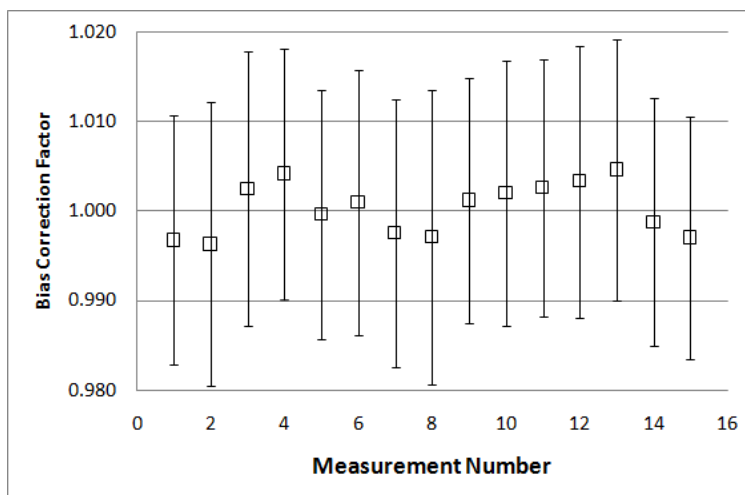


Figure B3: Plot of measured bias correction factors with standard uncertainties.

Assuming the bias correction factors follow a uniform distribution with a range as observed from the data, the best estimate of  $\beta$ , the maximum, minimum, and relative standard uncertainty are given in Table 1. Using a uniform distribution, the best estimate of  $\beta$ , the maximum, minimum, and relative uncertainty is given in Table B1.

Table B1  
Flow mixer and splitter bias correction factor statistics.

$\beta_o$	$\beta^+$	$\beta^-$	$u_\beta$
1.00044	1.0046	0.9963	2.4E-04

From these measurements, the bias correction factor is considered unity and the aerosol is considered well mixed. As a result, no correction to the direct comparison data has been made.